

Impact of Time-of-Flight and Point-Spread-Function for Respiratory Artifact Reduction in PET/CT Imaging: Focus on Standardized Uptake Value

Roya Sharifpour^{1,2}, Pardis Ghafarian^{3,4},
Mehrdad Bakhshayesh-Karam⁵, Hamidreza
Jamaati³, Mohammad Reza Ay^{1,2}

¹ Department of Medical Physics and Biomedical Engineering, Tehran University of Medical Sciences, Tehran, Iran, ² Research Center for Molecular and Cellular Imaging, Tehran University of Medical Sciences, Tehran, Iran, ³ Chronic Respiratory Diseases Research Center, National Research Institute of Tuberculosis and Lung Diseases (NRITLD), Shahid Beheshti University of Medical Sciences, Tehran, Iran, ⁴ PET/CT and Cyclotron Center, Masih Daneshvari Hospital, Shahid Beheshti University of Medical Sciences, Tehran, Iran, ⁵ Pediatric Respiratory Diseases Research Center, National Research Institute of Tuberculosis and Lung Diseases (NRITLD), Shahid Beheshti University of Medical Sciences, Tehran, Iran.

Received: 21 November 2016

Accepted: 24 February 2017

Correspondence to: Ghafarian P

Address: Chronic Respiratory Diseases Research Center, National Research Institute of Tuberculosis and Lung Diseases (NRITLD), Shahid Beheshti University of Medical Sciences, Tehran, Iran

Email address: pardis.ghafarian@sbmu.ac.ir

Background: The most important advantage of positron emission tomography/computed tomography (PET/CT) imaging is its capability of quantitative analysis. The aim of the current study was to choose the proper standardized uptake value (SUV) threshold, when the time-of-flight (TOF) and point spread function (PSF) were used for respiratory artifact reduction in the liver dome in a new-generation PET/CT scanner.

Materials and Methods: The current study was conducted using a National Electrical Manufacturers Association International Electrotechnical Commission body phantom, with activity ratios of 2:1 and 4:1. A total of 27 patients, with respiratory artifacts in the thorax region, were analyzed. PET images were retrospectively reconstructed using either a high definition (HD) + PSF (i.e., a routine protocol) algorithm or HD+PSF+TOF (PSF+TOF; i.e., to reduce the respiratory artifact) algorithms, with various reconstruction parameters. The SUV_{max} and SUV_{meanv} at different thresholds (i.e., at 45%, 50%, and 75%), were also assessed.

Results: Although in comparison to the routine protocol a higher SUV was observed when using the PSF+TOF method, this approach was used to reduce the respiratory artifact. The appropriate threshold for SUV was strongly related to the lesion size, reconstruction parameters, and activity ratio. The mean of the relative difference between PSF+TOF algorithm and routine protocol for SUV_{max} varied from 10.58±14.99% up to 35.49±32.60% (which was dependent on reconstruction parameters).

Conclusion: In comparison with other types of SUVs, the SUV_{max} value illustrated its significant overestimation, especially at the 4:1 activity ratio. The poor agreement between SUV_{max} and SUV_{50%} was also observed. When the TOF and PSF are utilized to reduce respiratory artifacts, the SUV_{50%} can be an accurate semi-quantitative parameter for PET/CT images, for all lesion sizes. For smaller lesions, however, a smaller filter size was required to observe an accurate SUV.

Key words: Standardized Uptake Value, Threshold, Time-of-Flight, Point-Spread-Function, PET/CT imaging, Respiratory artifact

INTRODUCTION

The quantitative assessment of ¹⁸F-fluorodeoxyglucose (¹⁸F-FDG) positron emission tomography/computed tomography (PET/CT) imaging is a noninvasive tool with

applications in oncology. Thus, metabolic and volumetric parameters lead to valuable data for patient monitoring and evaluation of therapy response (1-3). The standardized uptake value (SUV) is a semi-quantitative parameter,

which is widely used in evaluation of glucose metabolism, is prone to biological and technical factors (4-6). The SUVs, however, can vary depending on the method of reconstruction and parameters that are used (7-11). Thus, since PET images are obtained from different scanners, or even with different reconstruction methods in the same scanner, an accurate SUV is essential for reliable quantitative analysis. Previous studies have suggested different approaches to address reconstruction-dependent variation in SUVs (12-14). Furthermore, a more accurate SUV can be obtained with better spatial resolution (15, 16). The point spread function (PSF) has been used during PET reconstruction to improve the spatial resolution (17). Moreover, the time-of-flight (TOF) and PSF functions in new-generation PET/CT scanners lead to better lesion detectability, signal to noise ratio (SNR), spatial resolution, and uniformity (15, 16, 18-22). However, these techniques can also lead to higher SUVs (10, 11, 19, 23, 24). Isocontour thresholds, the sizes and shapes of the volume of interest (VOI), and various correction methods can provide different SUVs for the same lesion (7, 25-29). Previous studies have demonstrated that errors in the SUV measurement can lead to variations of up to 50% (4, 25, 26). In our previous study (30), we showed that, in the absence of gating devices, the TOF technique can reduce the respiratory artifact in the liver dome. In the current study, we aimed to extend our results by evaluating the combination of TOF and PSF with various reconstruction parameters to choose the optimal SUV threshold for clinical PET/CT images, for accurate quantification. This evaluation was performed to quantify PET/CT images with indices consisting of SUV_{max} and SUV_{mean} with various thresholds, in systematic phantom and patient studies.

MATERIALS AND METHODS

PET/CT Scanner

All measurements were performed on a Discovery 690 VCT (GE Healthcare, Milwaukee, USA) scanner, which was equipped with 64-slice CT (Light Speed VCT). The

58368 solid state detector elements of the CT scanner were arranged in 912 channels, in 64 rows. The PET component of the Discovery 690 VCT used $4.2 \times 6.3 \times 25$ mm³ lutetium-yttrium oxyorthosilicate (LYSO) crystals. The PET scanner consisted of 24 detector rings, with a 157 mm axial field of view (FOV). In the PET scanner, the timing resolution and coincidence time window of the TOF method were approximately 500 ps and 4.9 ns, respectively.

Phantom Study

A National Electrical Manufacturers Association (NEMA) International Electrotechnical Commission (IEC) Body Phantom was used in the current study. This phantom contained six spherical inserts (with internal diameters of 10, 13, 17, 22, 28, and 37 mm) to simulate tumors with different sizes, and one cylindrical insert to simulate the lung. The background of phantom was filled with 5.3 KBq/mL ¹⁸F-FDG solution. All spheres were filled with activity ratios of 4:1 and 2:1, relative to the background activity separately.

Patients Population

We retrospectively assessed 27 patients (i.e., 16 men and 11 women). The patients were the same as patient group in our previous study (30). The clinical indications for PET/CT examinations were as follows: lung cancer (n=4), non-Hodgkin's lymphoma (n=4), Hodgkin's lymphoma (n=3), colon cancer (n=2), renal cell carcinoma (n=4), pancreatic cancer (n=1), gastric cancer (n=1), breast cancer (n=3), esophageal cancer (n=4), and unknown primary cancer (n=1). A total of 75 lesions, located in the diaphragmatic region, including the lower lobe of the lungs, liver, spleen, and stomach, were assessed. The patients had an average age of 55 ± 15.21 years (range: 28–71 years). Patients with fasting blood sugar levels higher than 200 mg/dL were excluded from the current study. The fasting period was between 6 to 8 h. The PET/CT scan was performed 60.75 ± 1.48 min after an intravenous injection of 331.42 ± 71.03 MBq (range: 253–487 MBq) of ¹⁸F-FDG, according to the European Association of Nuclear Medicine guidelines (31).

Data Acquisition and Image Reconstruction

Following CT acquisition using smart mA technique, all emission data were obtained from the vertex to mid-thigh. PET images were reconstructed using a 256×256 image matrix, with 2.73 mm pixels, for the two main groups consisting of the routine protocol (with respiratory artifacts in the liver dome) and PSF+TOF (to reduce the artifacts). The VUE point high definition (HD) with PSF, (HD+PSF), was used as our routine protocol. The VUE point FX with PSF,(HD+PSF+TOF), was used as the PSF+TOF method. The reconstruction parameters used for our routine protocol were 3 iterations and 18 subsets, with a 6.4 mm Gaussian filter in full width at half maximum (FWHM). The PSF+TOF methods were reconstructed with 2 iterations, and 18 and 24 subsets, with 4.4, 5.4, and 6.4 mm FWHM post-smoothing filters.

Assessment Strategy

The current study aimed to obtain accurate quantification. For this purpose, the SUV_{max} (3D isocontour encompass the total lesion), and $SUV_{45\%}$, $SUV_{50\%}$, and $SUV_{75\%}$ (with the mean 3D isocontour values at 45%, 50%, and 75% of the maximum voxel value, respectively) were measured in the PET images. This was repeated for all reconstruction methods for both phantom and clinical data. The relative difference for all types of SUV and mean of difference in the SUV value for various reconstruction methods and routine protocol were also calculated.

Statistical Analysis

Statistical analyses were performed using SPSS packages (SPSS, version 22.0, Armonk, NY). The Shapiro-Wilk method was utilized to test for normality. A paired t-test was used for variables with a normal distribution, while a Wilcoxon signed ranks test was conducted on non-normally distributed data. The Lin concordance correlation coefficient (Lin CCC) was also applied to test the agreement between variables. Statistical significance was set at $p < 0.05$.

RESULTS

Figure 1 illustrates the comparison of the SUV_{max} , $SUV_{75\%}$, $SUV_{50\%}$, and $SUV_{45\%}$ of each sphere size, between various reconstruction protocols in the phantom study. Decreasing the VOI threshold, extended the underestimation of all types of SUV from the small sphere sizes to the larger sphere size. Thus, the underestimation of $SUV_{45\%}$ for all sphere sizes was observed in the NEMA phantom with the 2:1 activity ratio. Compared with other SUV types, the SUV_{max} was significantly overestimated during the 4:1 activity ratio. As in our previous work (30), the PSF+TOF3 (2 iterations, 18 subsets, and 6.4-mm post-filter) showed the lowest noise level and highest SNR among of all reconstruction methods used in the current study. Figure 2 illustrates the correlation between $SUV_{50\%}$ and SUV_{max} for all clinical data between PSF+TOF3 (2 iterations, 18 subsets, and 6.4-mm post-filter) and the other reconstruction methods. A noticeable variation was observed between the SUV_{max} and $SUV_{50\%}$ for all reconstruction parameters. The Lin CCC that was used is listed in Table 1. Prieto et al. (11) stated that, although the correlation could be a necessity, it may not be enough to ensure agreement of values for quantitative purposes. Thus, poor agreement between the SUV_{max} and $SUV_{50\%}$ (Lin CCC ≤ 0.90) of various reconstruction methods was seen. However, moderate, substantial, and almost perfect agreement was also observed (Lin CCC ≥ 0.90) between $SUV_{50\%}$ and SUV_{max} separately for each reconstruction method. In our clinical study, the mean of difference for various SUV thresholds between all reconstruction parameters and routine protocol is illustrated in Table 2. Decreasing the threshold diminished the differences, with a greater impact on small subset numbers and the larger post-smoothing filter. Figure 3 illustrates the lung window of CT images and PET images, with various reconstruction methods, of a typical patient with colon cancer. The reduction in the respiratory artifact was obvious when the PSF+TOF methods were applied. Furthermore, these methods led to a larger SUV_{max} , compared with the $SUV_{50\%}$ for all corresponding reconstruction methods. In comparison with the routine protocol, the hypermetabolic pulmonary nodules were more varied for the SUV_{max} versus $SUV_{50\%}$ for the other reconstruction methods.

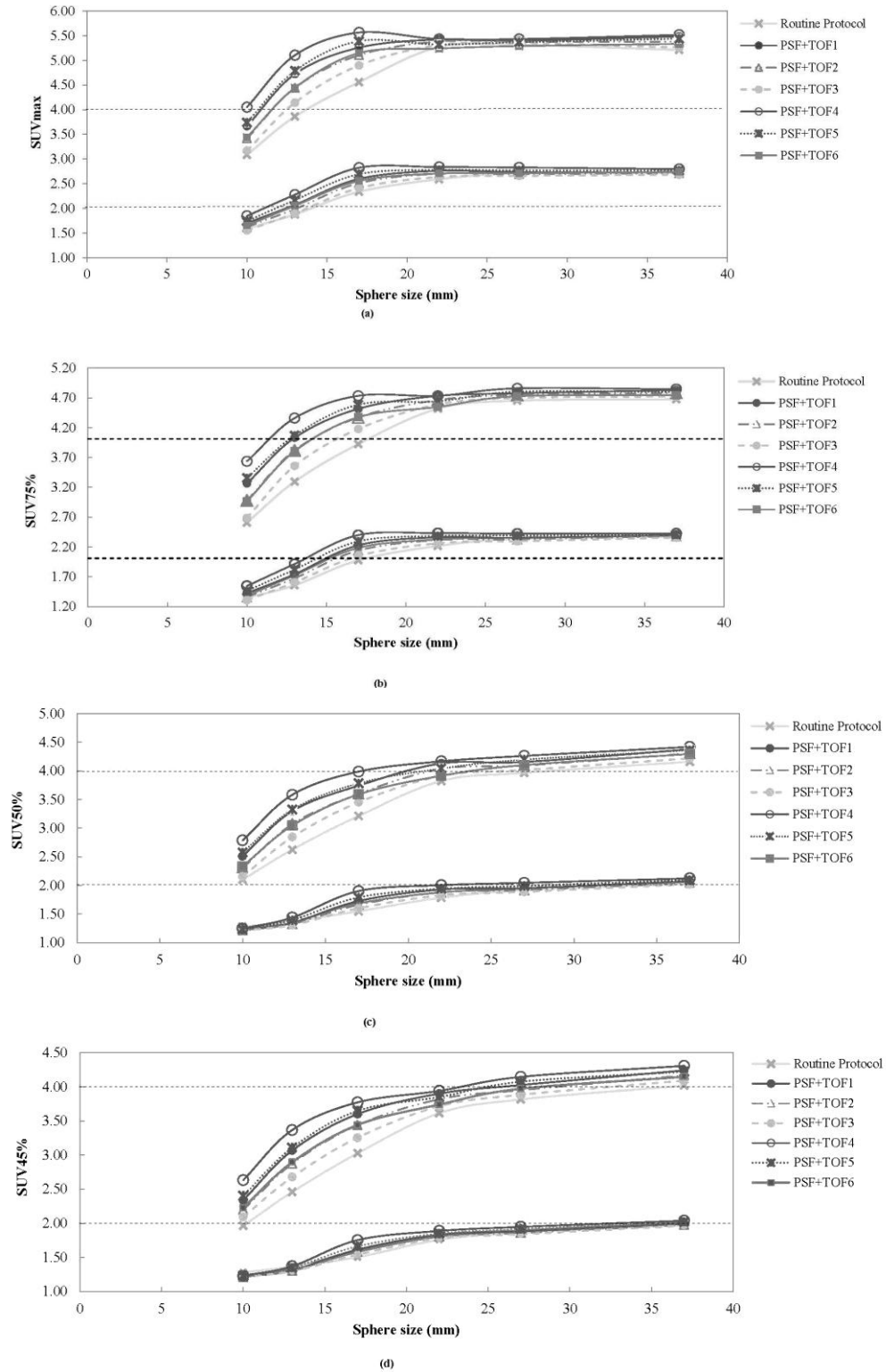


Figure 1. Illustration of measured (a) SUVmax, (b) SUV75%, (c) SUV50% and (d) SUV45% as a function of various sphere sizes in NEMA IEC Body phantom with 4:1 (upper) and 2:1 (lower) activity ratio and background concentration of 5.31 kBq/mL. Routine Protocol (HD+PSF with 3it, 18sub, 6.4mm filter), PSF+TOF1 (2it, 18sub, 4.4mm filter), PSF+TOF2 (2it, 18sub, 5.4mm filter), PSF+TOF3 (2it, 18sub, 6.4mm filter), PSF+TOF4 (2it, 24sub, 4.4mm filter), PSF+TOF5 (2it, 24sub, 5.4mm filter), PSF+TOF6 (2it, 24sub, 6.4mm filter).

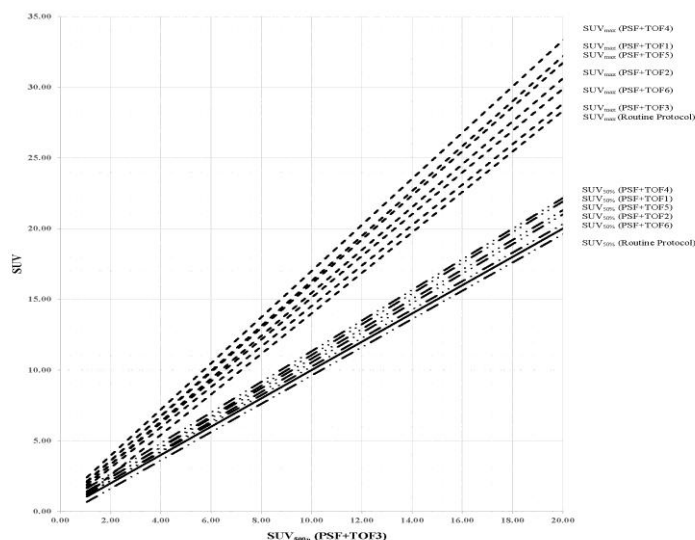


Figure 2.Correlation between measured SUV of 27 patients data. SUV50% with regard to PSF + TOF3 method is compared with the other reconstruction methods. The solid line shows the identity line. Routine Protocol (HD+PSF with 3it, 18sub,6.4mm filter), PSF+TOF1(2it, 18sub, 4.4mm filter), PSF+TOF2(2it, 18sub ,5.4mm filter), PSF+TOF3(2it, 18sub, 6.4mm filter), PSF+TOF4(2it, 24sub, 4.4mm filter), PSF+TOF5(2it, 24sub, 5.4mm filter), PSF+TOF6(2it, 24sub, 6.4mm filter).

Table 1.Lin concordance correlation coefficients Between the SUV Measured with Different Protocols

		SUV _{max}						SUV _{50%}							
		Routine Protocol	PSF+TOF1	PSF+TOF2	PSF+TOF3	PSF+TOF4	PSF+TOF5	PSF+TOF6	Routine Protocol	PSF+TOF1	PSF+TOF2	PSF+TOF3	PSF+TOF4	PSF+TOF5	PSF+TOF6
SUV _{max}	Routine Protocol	--	--	--	--	--	--	--	--	--	--	--	--	--	--
	PSF+TOF1	0.95	--	--	--	--	--	--	--	--	--	--	--	--	--
	PSF+TOF2	0.97	0.99	--	--	--	--	--	--	--	--	--	--	--	--
	PSF+TOF3	0.99	0.98	0.99	--	--	--	--	--	--	--	--	--	--	--
	PSF+TOF4	0.91	0.99	0.98	0.95	--	--	--	--	--	--	--	--	--	--
	PSF+TOF5	0.95	1.00	0.99	0.98	0.99	--	--	--	--	--	--	--	--	--
	PSF+TOF6	0.97	0.99	1.00	1.00	0.97	0.99	--	--	--	--	--	--	--	--
SUV _{50%}	Routine Protocol	0.84	0.70	0.74	0.79	0.65	0.70	0.75	--	--	--	--	--	--	--
	PSF+TOF1	0.92	0.82	0.86	0.90	0.77	0.82	0.87	0.95	--	--	--	--	--	--
	PSF+TOF2	0.89	0.77	0.82	0.86	0.73	0.78	0.83	0.97	0.99	--	--	--	--	--
	PSF+TOF3	0.86	0.73	0.78	0.83	0.68	0.73	0.79	0.99	0.98	0.99	--	--	--	--
	PSF+TOF4	0.92	0.84	0.87	0.91	0.80	0.84	0.89	0.92	0.99	0.98	0.96	--	--	--
	PSF+TOF5	0.90	0.79	0.84	0.88	0.75	0.80	0.85	0.95	1.00	1.00	0.98	0.99	--	--
	PSF+TOF6	0.87	0.75	0.80	0.84	0.71	0.76	0.81	0.98	0.99	1.00	1.00	0.98	0.99	--

Lin Concordance Correlation Coefficients (CCC) greater than 0.95 are in bold.

HD+PSF with 3it, 18sub and 6.4 mm filter

2it, 18sub, 4.4 mm filter

2it, 18sub, 5.4 mm filter

2it, 18sub, 6.4 mm filter

2it, 24sub, 4.4 mm filter

2it, 24sub, 5.4 mm filter

2it, 24sub, 6.4 mm filter

Table2. The Mean of Difference Between the SUV Measured with Various Protocols and Routine Protocol

Various Protocols	SUV	SUV _{max}	SUV _{75%}	SUV _{50%}	SUV _{45%}
PSF+TOF1 ^a		1.47±1.06	1.31±0.97	1.01±0.73	0.93±0.67
PSF+TOF2 ^b		1.00±0.77	0.87±0.66	0.68±0.54	0.64±0.48
PSF+TOF3 ^c		0.52±0.57	0.45±0.49	0.38±0.39	0.36±0.35
PSF+TOF4 ^d		1.95±1.43	1.74±1.33	1.28±0.93	1.21±0.89
PSF+TOF5 ^e		1.41±1.09	1.23±0.92	0.93±0.73	0.88±0.69
PSF+TOF6 ^f		0.88±0.89	0.73±0.68	0.58±0.56	0.55±0.51

- a. 2it, 18 sub, 4.4 mm filter.
- b. 2it, 18 sub, 5.4 mm filter.
- c. 2it, 18 sub, 6.4 mm filter.
- d. 2it, 24 sub, 4.4 mm filter.
- e. 2it, 24 sub, 5.4 mm filter.
- f. 2it, 24 sub, 6.4 mm filter.

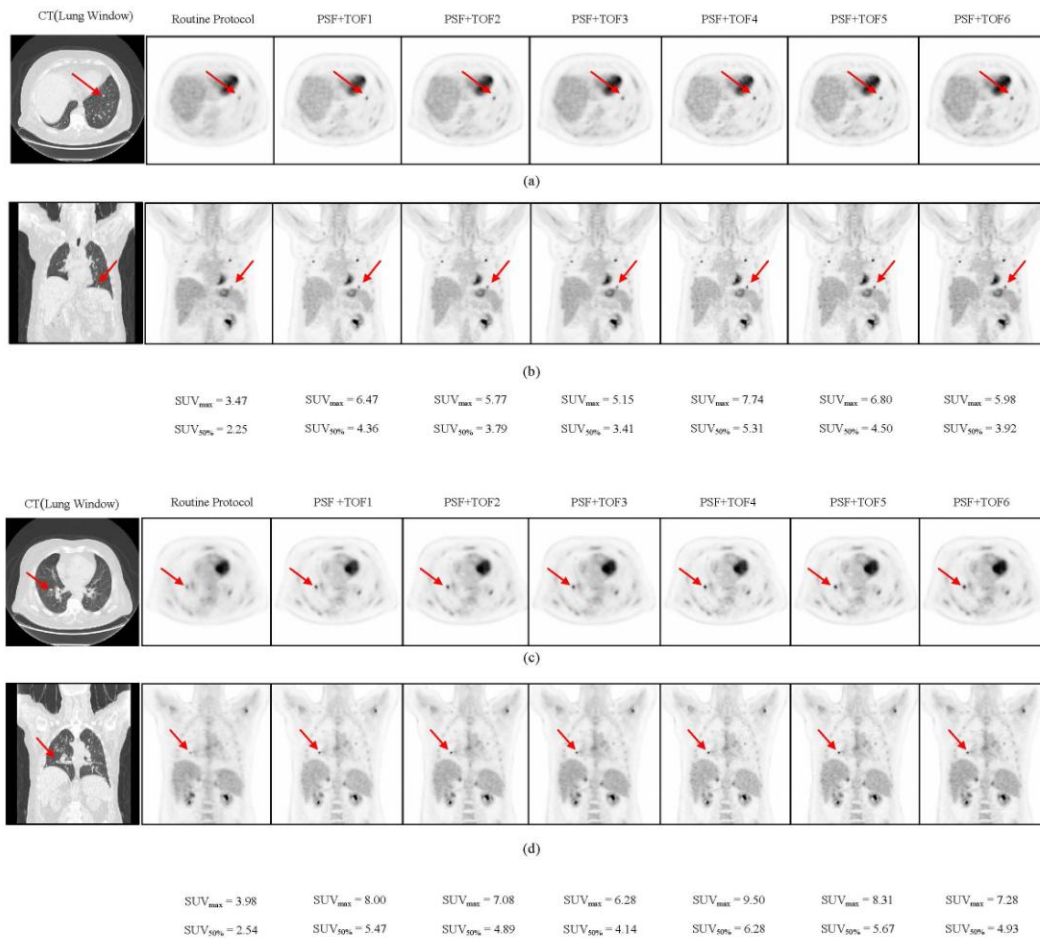


Figure3. Top (a,b) and bottom(c,d) pulmonary nodules of a patient with colon cancer. Transverse and coronal view for lung window of CT images and PET images with various reconstruction methods are illustrated. The impact of TOF on improvement in contrast and lesion detectability is clear in all methods. (Body weight: 105 kg and injected dose: 492MBq of ¹⁸F-FDG)

DISCUSSION

In the current study, we utilized a NEMA IEC body phantom to obtain the optimal SUV threshold for various sphere sizes and activity ratios, with various reconstruction methods (i.e., routine protocol and PSF+TOF). In the next step, the ability of various SUV thresholds to reduce the respiratory artifact was assessed in patients with different-sized lesions in the thorax region. Previous studies reported that using the PSF and TOF can lead to accurate quantitative analysis, with some SUV overestimation (10, 11). Thus, we obtained some optional reconstruction parameters to reach the acceptable image quality in oncology patients undergoing PET/CT imaging (21, 22). Variations in the reconstruction parameters and definition of the VOI for the SUV calculation can lead to discrepancies in the PET images properties and quantification analysis (28, 32). In the current study, we used SUV_{max} , $SUV_{75\%}$, $SUV_{50\%}$, and $SUV_{45\%}$, for the quantitative analysis of PET images. When a specific SUV threshold was applied, the use of different reconstruction methods did not significantly change the 2:1 and 4:1 activity ratios in the NEMA phantom, of the 22-, 28-, and 37-mm sized spheres. It should be noted, however, that when the VOI threshold decreased, the SUV underestimation was extended to a bigger sphere size in both activity ratios. For the 2:1 and 4:1 activity ratios, the underestimation of the SUV_{max} and $SUV_{75\%}$ occurred for sphere sizes up to 10 mm and 17 mm, respectively, while those for $SUV_{50\%}$ and $SUV_{45\%}$ occurred for spheres sized 22 and 17 mm, and 28 and 22 mm, respectively. The results of our phantom pertaining to the overestimation of the SUV_{max} corroborated with the findings of Prieto et al. (11), Boellaard (33), and Kelly and Declerck (12). The SUV_{max} is a popular quantification parameter, which is used in 91% of diagnostic reports (34). The overestimation of this quantitative parameter can be attributed to the high noise level in small voxel sizes and the Gibbs effect (slight enhancement of the edges due to PSF modeling) (11). Our results demonstrated that the SUV threshold was dependent on both the activity ratio and lesion size. The least variation in SUV, compared with the routine protocol, was observed for PSF+TOF3, while the second and third level belonged to PSF+TOF2 and PSF+TOF6 in the 4:1

activity ratio. Similar behavior was seen for all reconstruction methods for the 2:1 activity ratio. According to our phantom study, among all SUV threshold, the $SUV_{50\%}$ could be an accurate quantitative parameters for spheres sized 22, 28, and 37 mm, for both 2:1 and 4:1 activity ratios, regardless of the reconstruction methods. A $SUV_{50\%}$ with a smaller filter size and higher subset number is more appropriate for smaller sphere sizes for the 4:1 activity ratio. In general, all reconstruction parameters illustrated nearly the same behavior for all sphere sizes, when the $SUV_{50\%}$ was used for the 2:1 activity ratio. Our clinical data corroborated with our phantom study; decreasing the filter size and increasing the subset number produced a high SUV for all thresholds in various lesions (PSF+TOF4 illustrated the highest SUV). The current study demonstrated that the SUV_{max} and SUV with different thresholds were strongly dependent on reconstruction parameters that in line with previous study (35). This effect, however, was less pronounced when a larger filter size and smaller subset number were used. The mean of relative difference (data were not shown) between PSF+TOF algorithm and routine protocol for SUV_{max} varied from $10.58 \pm 14.99\%$ (PSF+TOF3; 2 iterations, 18 subsets, 6.4 mm post-filter) up to $35.49 \pm 32.60\%$ (PSF+TOF4; 2 iterations, 24 subsets, 4.4 mm post filter). It should be noted that although accurate SUVs were observed for small lesions when smaller filter sizes were used, it did not seem critical for larger lesion sizes. However, the $SUV_{50\%}$ displayed variation when different reconstruction methods were used; it is an accurate semi-quantitative parameter for PET/CT images when the TOF and PSF were used to reduce the respiratory artifact for all lesion sizes. A few limitations of our study should also be noted. Since we did not have a phantom that simulated the respiratory cycle, we utilized a stationary NEMA phantom. Furthermore, since there were no heavy and obese patients, the effect of various reconstruction parameters could not be evaluated in those groups of patients.

CONCLUSION

The PSF+TOF approach, with various reconstruction parameters produced higher SUVs (when compared with the routine protocol) and reduced the respiratory artifact in

the liver dome. The accurate estimation of the SUV was strongly dependent on reconstruction parameters, lesion size, and activity ratios. There was less variation in the SUV between PSF+TOF algorithms and routine protocol when a smaller subset number and larger filter size were used. Regardless of the reconstruction method, compared with other SUV types, the SUV_{50%} illustrated more accurate quantitative parameters for PET/CT images when the TOF and PSF were applied to reduce the respiratory artifact for larger lesion sizes. A smaller filter size needs to be properly applied for smaller lesions with a high activity ratio.

Abbreviations

Time of Flight=TOF; Point spread function=PSF; Positron emission tomography/Computed tomography=PET/CT; Standardized uptake value= SUV; ¹⁸F-fluorodeoxyglucose= ¹⁸F-FDG; Signal to noise ratio=SNR; Volume of interest=VOI; Lutetium-yttrium oxyorthosilicate=LYSO; Field of view=FOV; National Electrical Manufacturers Association=NEMA; International Electrotechnical Commission=IEC; European Association of Nuclear Medicine=EANM; High definition =HD; Full width at half maximum=FWHM; Lin concordance correlation coefficient=Lin CCC;

REFERENCES

1. Sheikhabaei S, Marcus C, Subramaniam RM. ¹⁸F FDG PET/CT and Head and Neck Cancer: Patient Management and Outcomes. *PET Clin* 2015;10(2):125-45.
2. Wahl RL, Jacene H, Kasamon Y, Lodge MA. From RECIST to PERCIST: Evolving Considerations for PET response criteria in solid tumors. *J Nucl Med* 2009;50 Suppl 1:122S-50S.
3. Young H, Baum R, Cremerius U, Herholz K, Hoekstra O, Lammertsma AA, et al. Measurement of clinical and subclinical tumour response using [18 F]-fluorodeoxyglucose and positron emission tomography: review and 1999 EORTC recommendations. *Eur J Cancer* 1999;35(13):1773-82.
4. Boellaard R. Standards for PET image acquisition and quantitative data analysis. *J Nucl Med* 2009;50 Suppl 1:11S-20S.
5. Adams MC, Turkington TG, Wilson JM, Wong TZ. A systematic review of the factors affecting accuracy of SUV measurements. *AJR Am J Roentgenol* 2010;195(2):310-20.
6. Vriens D, Visser EP, de Geus-Oei LF, Oyen WJ. Methodological considerations in quantification of oncological FDG PET studies. *Eur J Nucl Med Mol Imaging* 2010;37(7):1408-25.
7. Boellaard R, Krak NC, Hoekstra OS, Lammertsma AA. Effects of noise, image resolution, and ROI definition on the accuracy of standard uptake values: a simulation study. *J Nucl Med* 2004;45(9):1519-27.
8. Jaskowiak CJ, Bianco JA, Perlman SB, Fine JP. Influence of reconstruction iterations on ¹⁸F-FDG PET/CT standardized uptake values. *J Nucl Med* 2005;46(3):424-8.
9. Lodge MA, Chaudhry MA, Wahl RL. Noise considerations for PET quantification using maximum and peak standardized uptake value. *J Nucl Med* 2012;53(7):1041-7.
10. Akamatsu G, Mitsumoto K, Taniguchi T, Tsutsui Y, Baba S, Sasaki M. Influences of point-spread function and time-of-flight reconstructions on standardized uptake value of lymph node metastases in FDG-PET. *Eur J Radiol* 2014;83(1):226-30.
11. Prieto E, Domínguez-Prado I, García-Velloso MJ, Peñuelas I, Richter JÁ, Martí-Climent JM. Impact of time-of-flight and point-spread-function in SUV quantification for oncological PET. *Clin Nucl Med* 2013;38(2):103-9.
12. Kelly MD, Declerck JM. SUV_{ref}: reducing reconstruction-dependent variation in PET SUV. *EJNMMI Res* 2011;1(1):16.
13. Joshi A, Koeppe RA, Fessler JA. Reducing between scanner differences in multi-center PET studies. *Neuroimage* 2009;46(1):154-9.
14. Boellaard R, Oyen WJ, Hoekstra CJ, Hoekstra OS, Visser EP, Willemsen AT, et al. The Netherlands protocol for standardisation and quantification of FDG whole body PET studies in multi-centre trials. *Eur J Nucl Med Mol Imaging* 2008;35(12):2320-33.
15. Bettinardi V, Castiglioni I, De Bernardi E, Gilardi MC. PET quantification: strategies for partial volume correction. *Clinical and Translational Imaging* 2014;2(3):199-218.
16. Armstrong IS, Kelly MD, Williams HA, Matthews JC. Impact of point spread function modelling and time of flight on FDG

- uptake measurements in lung lesions using alternative filtering strategies. *EJNMMI Phys* 2014;1(1):99.
17. Sheikhabahaei S, Marcus C, Wray R, Rahmim A, Lodge MA, Subramaniam RM. Impact of point spread function reconstruction on quantitative 18F-FDG-PET/CT imaging parameters and inter-reader reproducibility in solid tumors. *Nucl Med Commun* 2016;37(3):288-96.
 18. Andersen FL, Klausen TL, Loft A, Beyer T, Holm S. Clinical evaluation of PET image reconstruction using a spatial resolution model. *Eur J Radiol* 2013;82(5):862-9.
 19. Kadrmaz DJ, Casey ME, Conti M, Jakoby BW, Lois C, Townsend DW. Impact of time-of-flight on PET tumor detection. *J Nucl Med* 2009;50(8):1315-23.
 20. Kadrmaz DJ, Casey ME, Black NF, Hamill JJ, Panin VY, Conti M. Experimental comparison of lesion detectability for four fully-3D PET reconstruction schemes. *IEEE Trans Med Imaging* 2009;28(4):523-34.
 21. Ahangari S, Ghafarian P, Shekari M, Ghadiri H, Bakhshayeshkaram M, Ay MR. The Impact of Point Spread Function Modeling on Scan Duration in PET Imaging. *Frontiers in Biomedical Technologies* 2015;2(3):137-45.
 22. Shekari M, Ghafarian P, Ahangari S, Ghadiri H, Bakhshayeshkaram M, Ay MR. Optimizing Image Reconstruction Parameters in Time of Flight PET/CT Imaging: a Phantom Study. *Frontiers in Biomedical Technologies* 2015;2(3):146-54.
 23. Jakoby BW, Bercier Y, Conti M, Casey ME, Bendriem B, Townsend DW. Physical and clinical performance of the mCT time-of-flight PET/CT scanner. *Phys Med Biol* 2011;56(8):2375-89.
 24. Bellevre D, Blanc Fournier C, Switsers O, Dugué AE, Levy C, Allouache D, et al. Staging the axilla in breast cancer patients with ¹⁸F-FDG PET: how small are the metastases that we can detect with new generation clinical PET systems? *Eur J Nucl Med Mol Imaging* 2014;41(6):1103-12.
 25. Vanderhoek M, Perlman SB, Jeraj R. Impact of different standardized uptake value measures on PET-based quantification of treatment response. *J Nucl Med* 2013;54(8):1188-94.
 26. Westerterp M, Pruijm J, Oyen W, Hoekstra O, Paans A, Visser E, et al. Quantification of FDG PET studies using standardised uptake values in multi-centre trials: effects of image reconstruction, resolution and ROI definition parameters. *Eur J Nucl Med Mol Imaging* 2007;34(3):392-404.
 27. Benz MR, Evilevitch V, Allen-Auerbach MS, Eilber FC, Phelps ME, Czernin J, et al. Treatment monitoring by 18F-FDG PET/CT in patients with sarcomas: interobserver variability of quantitative parameters in treatment-induced changes in histopathologically responding and nonresponding tumors. *J Nucl Med* 2008;49(7):1038-46.
 28. Makris NE, Huisman MC, Kinahan PE, Lammertsma AA, Boellaard R. Evaluation of strategies towards harmonization of FDG PET/CT studies in multicentre trials: comparison of scanner validation phantoms and data analysis procedures. *Eur J Nucl Med Mol Imaging* 2013;40(10):1507-15.
 29. Paquet N, Albert A, Foidart J, Hustinx R. Within-patient variability of (18)F-FDG: standardized uptake values in normal tissues. *J Nucl Med* 2004;45(5):784-8.
 30. Sharifpour R, Ghafarian P, Rahmim A, Ay MR. Quantification and reduction of respiratory induced artifacts in positron emission tomography/computed tomography using the time-of-flight technique. *Nucl Med Commun* 2017;38(11):948-955
 31. Boellaard R, Delgado-Bolton R, Oyen WJ, Giammarile F, Tatsch K, Eschner W, et al. FDG PET/CT: EANM procedure guidelines for tumour imaging: version 2.0. *Eur J Nucl Med Mol Imaging* 2015;42(2):328-54.
 32. Brendle C, Kupferschläger J, Nikolaou K, la Fougère C, Gatidis S, Pfannenbergl C. Is the standard uptake value (SUV) appropriate for quantification in clinical PET imaging? - Variability induced by different SUV measurements and varying reconstruction methods. *Eur J Radiol* 2015;84(1):158-162.
 33. Boellaard R. Need for standardization of 18F-FDG PET/CT for treatment response assessments. *J Nucl Med* 2011;52 Suppl 2:93S-100S.
 34. Beyer T, Czernin J, Freudenberg LS. Variations in clinical PET/CT operations: results of an international survey of active PET/CT users. *J Nucl Med* 2011;52(2):303-10.
 35. Shekari M, Ghafarian P, Ahangari S, Ay MR. Quantification of the impact of TOF and PSF on PET images using the noise-matching concept: clinical and phantom study. *Nuclear Science and Techniques* 2017;28(11):167.